

A comparative study between traditional topology optimization and lattice optimization for additive manufacturing

Evangelos Tyfloopoulos  | Martin Steinert

Department of Mechanical and Industrial Engineering, NTNU, Trondheim, Norway

Correspondence

Evangelos Tyfloopoulos, Department of Mechanical and Industrial Engineering, NTNU, Richard Birkelandsvei 2B, Trondheim 7034, Norway.
Email: evangelos.tyfloopoulos@ntnu.no

Abstract

Topology optimization (TO) aids designers to come up with new ideas that would be impossible to be designed without this technology. However, the optimized results are usually characterized by high geometric complexity, which makes almost impossible their manufacturing by conventional methods. Additive manufacturing (AM) overcomes this problem and increases the design flexibility. In addition, lattice structures with their porous infill combine the design flexibility with good material properties, such as high strength compared with relatively low mass. In this paper, the authors compare designs derived from traditional TO lattice optimization with respect to their tensile strength. A case study of a custom cylindrical model is used to support the theory and collect empirical data. The simulation data as well as the implemented methodology in this work can be used as a guidance for the designers looking for new lightweight design ideas for AM.

KEY WORDS

additive manufacturing, finite element analysis, lattice optimization, topology optimization

1 | INTRODUCTION

In this paper, a case study of a custom cylindrical model, with four alternative geometries, was developed and used to compare the derived results from both traditional compliance topology optimization (TO) and lattice optimization with respect to tensile stress.

On the one hand, compliance TO is the most common case of TO, because of the fact that it is mechanically intuitive (work done by the loads) and self-adjoint.^{1,2} In general, structural TO can combine size, shape, and TO in order to identify the best solution of a structure minimizing/maximizing an objective function with respect to design constraints.³ However, the traditional TO does not usually take under consideration fatigue, buckling, or other nonlinear types of analysis.⁴ In addition, it still has some clear limitations even with the use of additive manufacturing (AM) construction methods. One important limitation is that the optimized designs change the original shape, unless the designer uses many constraints that can “freeze” the external shape of the structure. Furthermore, the general TO problem discretizes the design space in elements with relative densities between 1 (solid) and 0 (void).⁵ This, in its turn, results to large intermediate relative densities that the traditional algorithms cannot take into advantage. Finally, the

This is an open access article under the terms of the Creative Commons Attribution License, which permits use, distribution and reproduction in any medium, provided the original work is properly cited.

© 2019 The Authors. Material Design & Processing Communications published by John Wiley & Sons Ltd

optimized designs can contain overhang structures. These structures need to be redesigned in order to avoid stress concentrations and support material in 3D printing.⁶

On the other hand, lattice structures are of high interest in AM nowadays because of their mechanical properties and design flexibility.⁷ According to Gibson and Ashby,⁸ lattice structures are repetitive cellular structures that constitute a subcategory of the so-called architected or hybrid materials. Architected materials are considered all the combinations that consist of either two or more materials such as metals, polymers, elastomers, glasses, and ceramics or one material and void. The different combinations of these materials affect both the physical and mechanical properties of the architected materials and thus the end structure.⁹ Cellular structures, in their turn, according to Gibson and Ashby,⁸ can be described as assemblies that consist of cells with either solid edges or faces and can be classified in honeycombs and open/closed-cell foams, which are 2D and 3D structures, respectively. Honeycombs are 2D cellular designs, such as the most known hexagonal honeycomb, that can be extruded in the third direction. Open-cell and closed-cell foams are 3D cellular designs where only cell edges and cell faces are shown, respectively. In these three categories, lattices can also be added. The appearance of lattices is similar to open-cell foams when six or more unit cells are used in each direction. However, they differ in that they are stretch dominated comparing with the open-cell foams, which are mainly bending-dominated structures.^{10,11} In general, nature and mathematics have inspired designers both in design and product development. In particular, designers mimic different porous structures found in nature and try to benefit from their lightweight composition and robustness. Some examples of these structures are bones,¹² shells,¹³ and wood.¹¹

The lattice infill of the structures is mainly constructed by a slicing software before the creation of the g-code, which is sent to the 3D printer. Alternatively, the lattice infills are generated by parametric equations using a computer algebraic system such as Matlab⁴ or can be directly modeled using pattern features in a CAD software.¹⁴ Recently, lattice TO has been developed in order to overcome the aforementioned limitations of the traditional TO by preserving the original structure's shape and exploiting the intermediate relative densities using exact optimal densities taken by the optimization.⁶

The most crucial part in lattice optimization is the calculation of the macroscopic (effective) material properties of the structures, on the basis of the representative volume element (RVE), which is used to create the lattice infill. In literature, there are three different approaches that try to confront this problem; homogenization, continuum modeling, and member modeling.

Homogenization is considered as the most common approach. This method is based on the micromechanics theory, which uses scaling laws to calculate the effective (macroscopic) elastic properties of the heterogeneous materials. In other words, the RVE is used in a finite element analysis (FEA) to predict the effective material properties using periodic boundary conditions. Finally, these material properties can be adapted to the whole lattice structure.⁶

The continuum modeling approach uses bulk material properties to describe the microscopic material properties of the structure. This method is independent of the lattice type, size, and contact effects and thus does not take into account the material anisotropy created by the AM methods.¹⁵

Finally, the member modeling invokes the beam theory to represent and describe the microscopic properties and build them up as properties of the whole cellular structures.¹⁶ All these approaches have their advantages and disadvantages, and they need to be experimentally validated. In this paper, the homogenization method will be employed.

2 | METHODS AND RESULTS

A flowchart of the implemented phases in this research paper is illustrated in Figure 1. The design and the numerical parts were conducted in SolidWorks 2019 and ANSYS R1 software, respectively.

A cylindrical 3D model with four design alternatives was used as a case study in this paper. The different design alternatives were Geometry 1—Original, Geometry 2—Topology, Geometry 3—Cubic, and Geometry 4—Octahedral (diamond), as shown in Figure 2C.

The first design alternative (Geometry 1—Original) was designed at SolidWorks and then imported to ANSYS Workbench for the TOs (see Figure 2A). The initial design was developed in a way that it could be 3D printed and eventually tested for tensile/compression in a future experiment. As it is shown on Figure 2B, the model's geometry consists of five bodies. Bodies 1 and 5 are the areas where the grippers of a tensile test machine can be applied. Bodies 2 and 4 were used as transition from the solid to lattice areas in order to avoid material failures at gripper's area. Finally, body 3 is the design space of the model, which was used for optimization with 50% mass reduction as constraint. A higher

FIGURE 1 A schematic overview of the used procedure

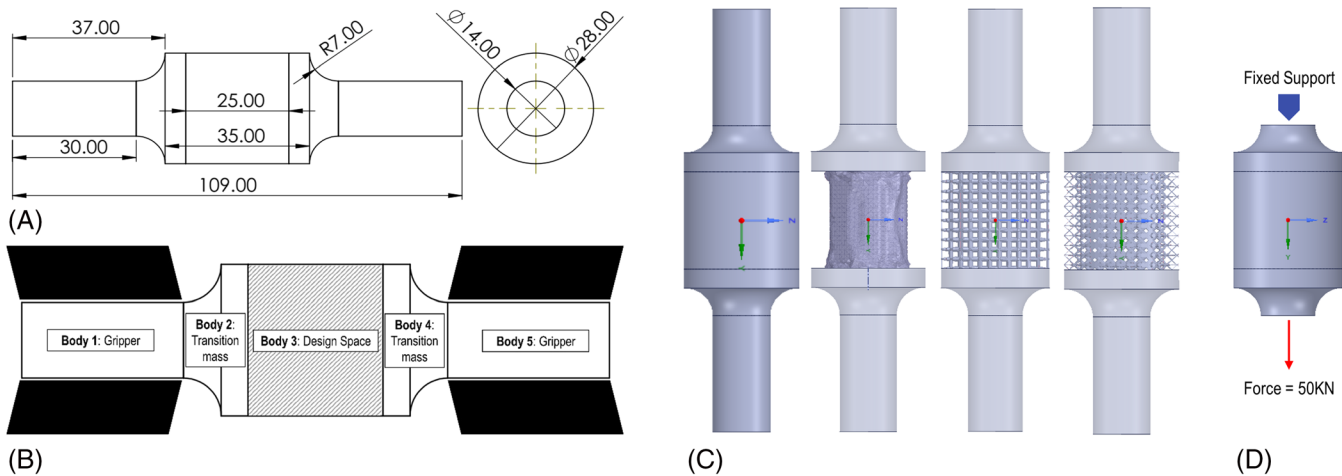
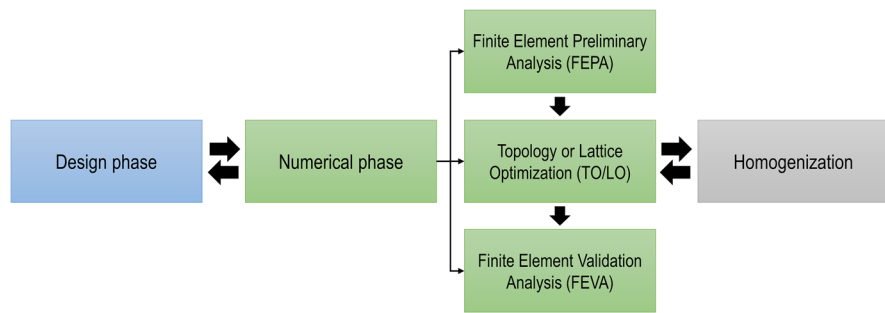


FIGURE 2 (A) The initial design; (B) the five bodies of the model; (C) the four geometries from left to right: Geometry 1—Original, Geometry 2—Topology, Geometry 3—Cubic, and Geometry 4—Octahedral; and (D) the used boundary conditions

diameter in this area was chosen in order to increase the design space for the TO algorithm. According to their designs, the authors expect that the specimens will break in the middle of body 3. A future tensile experiment could validate this assumption.

The numerical part in this paper consists of three phases: the finite element preliminary analysis of the model (FEPA), the topology or lattice optimization (TO/LO), and the finite element validation analysis (FEVA). The used boundary conditions, in all the aforementioned numerical phases, were based on a tensile test. Hence, a fixed constraint was applied on the one side of the model and a ramped force, $F = 50\text{ kN}$, on the other one. The gripper areas were excluded from the FEA as it is illustrated on Figure 2D. A structural ASTM A36 steel was assigned to the 3D model with the following properties; $E = 200\,000 \text{ MPa}$, $\nu = 0.3$, $\rho = 7.85 \text{ g/cm}^3$, yield strength = 250 MPa, and ultimate strength = 460 MPa. The second design alternative (Geometry 2—Topology) was topology optimized with the use of TO with compliance as objective function and 50% mass reduction of the design space as design constraint.

The third and fourth geometries (Geometry 3—Cubic and Geometry 4—Octahedral) are the results of LO with 50% mass design constraint, consisting of cubic and octahedral lattice cell types, respectively. The conducted LO at ANSYS is based on the homogenization method presented in the paper of Cheng et al.⁶ Interested readers should refer to that work for further details. In the first place, the software identifies the optimal lattice density of the design space using the homogenization approach, as well as the TO theory, with respect to the given objective function and design constraints. Subsequently, the designer has to choose both the cell type, the size, and the density limits of the lattice structure. On the one hand, the lower density limit was used in order to avoid too thin lattices in the structure. On the other hand, the elements with a density higher than the upper limit are considered as solid structure. Finally, the initial structure was reconstructed by placing lattice cells with varying densities, and thus varying material properties, inside the derived lattice density. Especially for the latter two geometries, the variable density of the lattices was chosen between 0.1 and 0.6, and their cell size was defined as equal to 2.5 mm. Furthermore, the surface of body 3 (design space) was

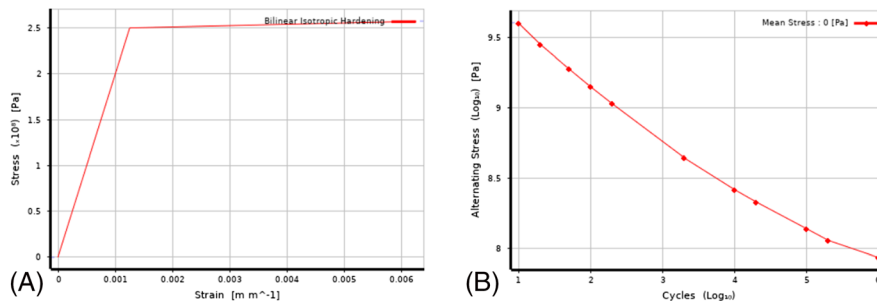


FIGURE 3 The nonlinear and fatigue behavior of the structural ASTM A36 steel: (A) the stress-strain curve and (B) the S-N curve

TABLE 1 The results of the numerical phase

Geometries	Number of Nodes/Elements	Mass of 3D Models (Body 3/Total), kg	Mass Reduction (Body 3/Total), %	Compliance, N/mm	Equivalent Plastic Strain
Geometry 1—Original	2377780/1754292	0.121/0.267	-	-	0.0009
Geometry 2—Topology	1185833/867768	0.060/0.206	50.5/22.8	0.036	0.0015
Geometry 3—Cubic	1206319/730011	0.049/0.195	59.8/27.0	0.082	1.4791
Geometry 4—Octahedral	1345770/758734	0.047/0.193	61.3/27.7	0.057	0.0010

excluded from the optimization. The reason for that was to take into account the powder removal from the inside of the lattice structure, in case that selective laser melting (SLM) would be selected as AM method for the specimens.

At the FEVA, a nonlinear validation analysis was implemented in each of the design alternatives. The nonlinear and fatigue behavior of the assigned material (structural ASTM A36 steel) is depicted on Figure 3. A mesh control was applied to their design space (body 3) with 0.5-mm element size, in order to create a proper mesh quality at the lattice structures. This led to a huge number of elements (see Table 1) and increased dramatically the simulation time. For this reason, only 10 steps were used to conduct the nonlinear validation analysis. In addition to geometries' compliance found at the optimization phase, their equivalent plastic strain was calculated here, in order to identify and compare their nonlinear tensile behavior.

Table 1 shows the mass, mass reduction, compliance, and equivalent plastic strain for each of the four geometries. The conducted optimizations at ANSYS could reduce the mass of the design space of geometries 2, 3, and 4 by 50.5%, 59.8%, and 61.3%, respectively, and not by 50% as it was chosen as design constraint. This happened because of geometric differences between the lattice density and the reconstructed lattice geometry by the software's algorithm. According to the compliance results of the optimized geometries, the Geometry 2—Topology was the stiffest with compliance equal to 0.036 N/mm compared with Geometry 3—Cubic and Geometry 4—Octahedral with 0.082 and 0.057, respectively. It seems that the cubic and the octahedral lattice structures are two and three times weaker than the topology-optimized design.

However, the results of the equivalent plastic strain derived from the validation studies showed something different. On the basis of these results, the strongest structure was the Geometry 4—Octahedral with the lowest plastic strain equal to 0.0010, which is at the same level with the equivalent plastic strain of the initial design (Geometry 1—Original). The Geometry 2—Topology came at second place with a plastic strain 0.0015 and finally the Geometry 3—Cubic with the highest plastic strain equal to 1.4791.

3 | CONCLUSIONS

A comparison study of four design alternatives of a cylindrical model, which was used as a case study, was conducted in this paper. The used geometries were the original, a topology-optimized geometry, and two geometries that contained

cubic and octahedral (diamond) lattice structure in the middle, generated by LO. The compliance results were different compared with the equivalent plastic strain found in the validation analysis. This proves that the topology/lattice optimized designs are oriented to the given load cases and analysis types. Thus, the optimized designs cannot be expected to show the same behavior at the nonlinear area. Hence, there is a clear need for further investigation of the optimized designs before the final decision. In other words, it is possible to choose an optimized solution that does not have the lowest compliance, such as the Geometry 3—Octahedral in this paper, but has shown a better nonlinear or fatigue behavior.

The lattice structures together with the LO can either replace or be integrated in the traditional TO method. Especially in the case where the structure's layout has to be preserved, the LO may be preferred over the TO. However, an extensive research has to be carried out in the pursuit of the lattice structure that gives the best design solution for specified load cases of a structure.

As future work, the execution of experimental validations of the design alternatives was decided by the authors. Thus, the four geometries will be manufactured with an MLS 3D-printer, and then they will be tested for tension. A comparison study between the simulation and experimental results could be of high interest. Finally, the porosity of the 3D-printed specimens could be calculated by a scanning electron microscopy (SEM) analysis. The specimens' porosity, in its turn, could be used as evaluation criterion for the 3D printing efficiency. Finally, in addition to the tensile test, fatigue, buckling, or other nonlinear tests could be implemented.

ACKNOWLEDGMENT

The authors would like to thank Georgios Michailidis for his help and support during the conduct of this research.

ORCID

Evangelos Tyflopoulos  <https://orcid.org/0000-0001-9289-6163>

REFERENCES

1. Bendsøe MP. Optimal shape design as a material distribution problem. *Struct Optim*. 1989;1(4):193-202. <https://doi.org/10.1007/BF01650949>
2. Christensen PW, Klarbring A. An Introduction to Structural Optimization: Springer Science & Business Media; 2008. <https://doi.org/10.1007/978-1-4020-8666-3>.
3. Bendsøe MP, Sigmund O. *Topology Optimization: Theory, Methods, and Applications*. Berlin; New York: Springer; 2003. xiv, 370 p. <https://doi.org/10.1007/978-3-662-05086-6>.
4. Clausen A, Aage N, Sigmund O. Exploiting additive manufacturing infill in topology optimization for improved buckling load. *Engineering*. 2016;2(2):250-257. <https://doi.org/10.1016/J.ENG.2016.02.006>
5. Zhou M, Rozvany GIN. The COC algorithm, part II: topological, geometrical and generalized shape optimization. *Comput Methods Appl Mech Eng*. 1991;89(1-3):309-336. [https://doi.org/10.1016/0045-7825\(91\)90046-9](https://doi.org/10.1016/0045-7825(91)90046-9)
6. Cheng L, Zhang P, Biyikli E, Bai J, Robbins J, To A. Efficient design optimization of variable-density cellular structures for additive manufacturing: theory and experimental validation. *Rapid Prototyp J*. 2017;23(4):660-677. <https://doi.org/10.1108/RPJ-04-2016-0069>
7. Liu J, Gaynor AT, Chen S, et al. Current and future trends in topology optimization for additive manufacturing. *Struct Multidiscip Optim*. 2018;57(6):2457-2483. <https://doi.org/10.1007/s00158-018-1994-3>
8. Gibson LJ, Ashby MF. *Cellular Solids: Structure and Properties*. Cambridge, England: Cambridge University Press; 1999. <https://doi.org/10.1017/CBO9781139878326>.
9. Ashby MF. Designing architected materials. *Scr Mater*. 2013;68(1):4-7. <https://doi.org/10.1016/j.scriptamat.2012.04.033>
10. Ashby MF. The properties of foams and lattices. *Phil Trans Math Phys Eng Sci*. 2005;364(1838):15-30. <https://doi.org/10.1098/rsta.2005.1678>
11. Ad P, Broeckhoven C, Yadroitseva I, et al. Beautiful and functional: a review of biomimetic design in additive manufacturing. *Addit Manuf*. 2019;27:408-427. <https://doi.org/10.1016/j.addma.2019.03.033>
12. Wu J, Aage N, Westermann R, Sigmund O. Infill optimization for additive manufacturing—approaching bone-like porous structures. *IEEE Trans Vis Comput Graph*. 2018;24(2):1127-1140. <https://doi.org/10.1109/TVCG.2017.2655523>
13. Jia Z, Wang L. 3D printing of biomimetic composites with improved fracture toughness. *Acta Materialia*, Inc 2018, <https://ssrn.com/abstract=3300049>.
14. Yan C, Hao L, Hussein A, Raymont D. Evaluations of cellular lattice structures manufactured using selective laser melting. *Int J Mach Tool Manuf*. 2012;62:32-38. <https://doi.org/10.1016/j.ijmachtools.2012.06.002>
15. Correa DM, Klatt T, Cortes S, Haberman M, Kovar D, Seepersad C. Negative stiffness honeycombs for recoverable shock isolation. *Rapid Prototyp J*. 2015;21(2):193-200. <https://doi.org/10.1108/RPJ-12-2014-0182>
16. Ahmadi S, Campoli G, Yavari SA, et al. Mechanical behavior of regular open-cell porous biomaterials made of diamond lattice unit cells. *J Mech Behav Biomed Mater*. 2014;34:106-115. <https://doi.org/10.1016/j.jmbbm.2014.02.003>

How to cite this article: Tyflopoulos E, Steinert M. A comparative study between traditional topology optimization and lattice optimization for additive manufacturing. *Mat Design Process Comm.* 2019;e128. <https://doi.org/10.1002/mdp2.128>